

Cell Size Dependence of Threshold Conditions for the Delineation of Drainage Networks from Gridded Elevation Data

P. Tarolli¹, G. Dalla Fontana¹, G. Moretti², S. Orlandini²

¹Department of Land and Agroforest Environments, University of Padova, Agripolis,
Viale dell'Università, 16 – 35020 Legnaro (Padova), Italy
Telephone: +39 049 827 2695
Fax: +39 049 827 2686
Email: paolo.tarolli@unipd.it, giancarlo.dallafontana@unipd.it

²Department of Mechanical & Civil Engineering, University of Modena & Reggio Emilia,
Via Vignolese, 905 – 41100 Modena, Italy
Telephone: +39 059 205 6105
Fax: +39 059 205 6126
Email: giovanni.moretti@unimore.it, stefano.orlandini@unimore.it

1. Introduction

The drainage network is the pattern of tributaries and master streams in a drainage basin as delineated on a planimetric map. In theory, the network includes all the minor rills which are definite watercourses, even including all the ephemeral channels in the furthestmost headwaters. In practice, the detail of the drainage network is dependent on the scale of the map used to trace the channels (Leopold et al. 1964, p. 131). When preparing a topographic map the headward limits of the blue lines do not reflect any statistical characteristic of streamflow occurrence, nor differences in the hydrologic response of the headwater due to the various combinations of climate, topography and geology. In actual fact, they are drawn to fit a rather personalized aesthetic (Leopold 1994, p. 228). However, in light of recent field studies on the channel head (e.g., Dietrich and Dunne 1993), of increasing availability of accurate digital elevation data due to the LiDAR (Light Detection And Ranging) technology (e.g., Tarolli and Tarboton, 2006; Carter et al. 2007; Cavalli et al. 2008; Vianello et al. 2009; Tarolli and Dalla Fontana 2009), and of recent advances in terrain analysis (e.g., Gallant and Wilson 2000; Moretti and Orlandini 2008; Orlandini and Moretti 2009), a rationale for the delineation of drainage networks can be sought.

A field definition of the channel head is provided by Dietrich and Dunne (1993) as the upstream boundary of concentrated water flow and sediment transport between definable banks. Although it is not easy to provide a globally useful criterion for a well-defined bank, it is commonly accepted that the bank is recognizable as a morphological feature independent of the flow. In this perspective, a detailed description of hydrologic flows may not be required in order to predict channel heads, and meaningful predictive models can be formulated by combining terrain analysis and generalizations from field facts. Field and theoretical studies addressing the problem of defining where channels begin have led to the definition of different threshold conditions for channel initiation. O'Callaghan and Mark (1984) and Tarboton et al. (1988) defined channel networks on a digital elevation model as those pixels that have an accumulated drainage area greater than some "threshold support area." Montgomery and Dietrich (1988) proposed to use a threshold on a power function of both drainage area and the local slope. Howard (1994) considered a threshold on the gradient divergence normalized by mean gradient. Peckham (1995) investigated a method based

on Strahler's (1957) classification of drainage networks extracted from digital elevation data, and iterated pruning of exterior links.

In the present study, these criteria are evaluated by using accurate field observations of channel heads and channel network in the Rio Cordon catchment (Eastern Italian Alps, Fig. 1), gridded elevation data obtained from high-precision LiDAR surveys (Cavalli et al. 2008), and advanced methods for the delineation of drainage basins and surface flow paths from these data (Orlandini et al. 2003; Orlandini and Moretti 2009). The dependence of threshold conditions for the delineation of drainage networks on the size of grid cells involved is investigated.

2. Methods

Surface flow paths are determined by using the D8 and D8-LTD single flow direction algorithms (O'Callaghan and Mark 1984; Orlandini et al. 2003; Orlandini and Moretti 2009). In Orlandini and Moretti (2009) the D8-LTD method is found to provide a sounder description of surface flow paths than multiple flow direction algorithms. The D8-LTD method is therefore preferred in this study over other flow direction algorithms, and the capabilities of this method over the simpler and still commonly used D8 method are highlighted. The D8-LTD (eight flow directions, least transverse deviation) method performs a path-based analysis in which the deviations between steepest and possible flow directions are accumulated along the path and not just evaluated at the local scale as made by the D8 method. Transverse deviations are used to provide an accurate path-based analysis and this explains the name given to the method. A detailed description of the D8-LTD method can be found in Orlandini et al. (2003) and Orlandini and Moretti (2009).

Five criteria for the automated identification of channel heads from gridded elevation data are evaluated in this study. Each of these criteria defines a threshold condition for channel initiation and assumes that channels originate where threshold exceedences occur. Thresholds are given in terms of (1) drainage area A as proposed by O'Callaghan and Mark (1984) and Tarboton et al. (1988), (2) slope area function AS^k as proposed by Montgomery and Dietrich (1988), (3) gradient divergence normalized by mean gradient D as proposed by Howard (1994), (4) Strahler order SO of the drainage network extracted from gridded elevation data as proposed by Peckham (1995), and (5) Horton order HO of the drainage network extracted from gridded A elevation data (Horton 1945; Strahler 1957). It is specified that the drainage area A at a given cell is computed by accumulating local contributions along the upslope drainage system. The slope S at a given cell is evaluated along the flow direction towards its downslope neighbor, and it is conventionally assumed to be positive downward. The gradient divergence D is computed as the total curvature divided by mean gradient positive upward. Some details on the implementation of these criteria are provided here. A two-step procedure is used to determine the drainage network from criteria (4) and (5). In the first step, Strahler classification is applied to all the surface flow paths, including those generated at the source cells of the DTM. A surface flow path order (SFPO) is assigned to each link between a source and a junction or between junctions. In the second step, surface flow paths having order less than or equal to a given threshold (SFPO_t) are filtered. The remaining surface flow paths are assumed to provide predictions of the channels forming the drainage network. Channel orders (CO) in the obtained drainage network are computed as $CO = SFPO - SFPO_t$.

3. Case Study

The Rio di Col Duro basin, a sub-basin of Rio Cordon, is located in the Dolomites, a mountain region in the Eastern Italian Alps (Fig. 1). The area of the Rio di Col Duro basin is about 0.5 km². The elevation ranges from 1935 to 2385 m above sea level (asl) with an average of 2199 m asl. The slope angle is 25° in average, and 74° at maximum. The area has a typical Alpine climate with a mean annual rainfall of about 1100 mm. Precipitation occurs mainly as snowfall from November to April. Runoff is dominated by snowmelt in May and June, but summer and early autumn floods represent an important contribution to the flow regime. During summer, storm events and long dry spells are common. During these events several shallow landslides are triggered on steep screes at the base of cliffs (Tarolli et al., 2008). Soil thickness varies between 0.2 and 0.5 m on topographic spurs to depths of up to 1.5 m on topographic hollows. The vegetation covers the 97% of the area and consists in high altitude grassland (91%), and sporadic tall forest (6%). The remaining 3% of the area is unvegetated talus deposits. The geological settings of the basin are rather complex: sandstones and calcareous-marly rocks crop out; moraines, scree deposits and landslide accumulations are also widespread. Differently from many Alpine torrents, in which control works such as check dams and channel lining have extensively been built, no artificial structures are present in the headwaters of the Rio di Col Duro, where channels develop their morphology in response to loads of water and sediments imposed on them, reflecting ultimately the natural interaction between climate and geology. A picture of the study area showing the junction of Rio di Col Duro with Rio Cordon is provided in Fig. 2.

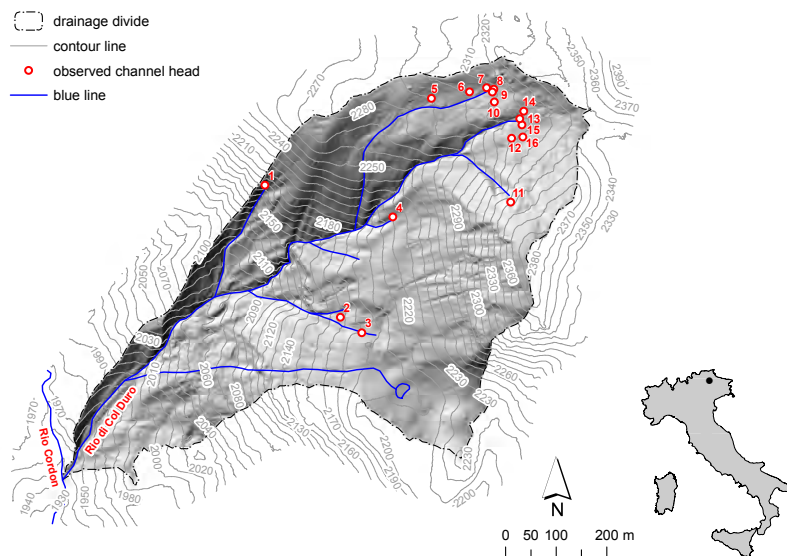


Figure 1. Topographic map of the Rio di Col Duro drainage basin showing observed channel heads, numbered progressively from left to right, and related blue lines. The location of the study area is also shown on the right hand side.

Several field surveys were conducted during the past few years including a LiDAR survey carried out during snow free conditions in October 2006. A recent campaign carried out in September–October 2008 has provided additional details on field-mapped channels and channel heads. Field surveys were carried out along the entire drainage network. The area was systematically walked along all drainage lines up to the catchment divide. Sixteen channel heads were mapped with an accuracy of a few

centimetres using a differential global positioning system (DGPS). The channel head or first-order stream head was defined as the point at which non-confined divergent flows on the hillslope converge to a drainage line with a well-defined flow path, i.e., the upstream limit of concentrated flow (Dietrich and Dunne 1993). The width of surveyed channels at the bankfull stage was found to range from 1 to 5 m.



Figure 2. Picture of the study area showing the junction of Rio di Col Duro with Rio Cordon.

LiDAR data and high resolution aerial photographs were acquired from a helicopter using an airborne laser terrain mapper (ALTM) 3100 OPTECH, and Rollei H20 Digital camera flying at an average altitude of 1000 m above ground level (agl) during snow free conditions in October 2006. The flying speed was 80 knots, the scan angle 20° and the pulse rate 71 kHz. The survey design point density was approximately 7 points/m², recording up to 4 returns, including first and last. LiDAR point measurements were filtered into returns from vegetation and bare ground using the TerrascanTM software classification routines and algorithms. The vertical accuracy, evaluated by a direct comparison between LiDAR and ground DGPS elevation points, was estimated to be less than 0.2 m (RMSE), an acceptable value for LiDAR analyses in the field of geomorphology (Mckean and Roering 2004; Glenn et al. 2006; Frankel and Dolan 2007; Tarolli and Dalla Fontana 2009).

The LiDAR bare ground dataset was used to generate an accurate 1-m resolution digital terrain model (DTM). Among the techniques for interpolation proposed in the literature, the natural neighbour technique was selected. This technique was found to provide accurate gridded elevation data from regular, sparse, clustered or random combinations of distributions of points (Sibson 1981). In addition, such interpolator is expected to produce smaller smoothing effects than other methodologies such as spline or kriging. This is a desirable property since a rough morphology representation is able to detect small convergences/depressions that are critical for the recognition of morphological features such as channels. Natural neighbour uses the ratio between the Voronoi tassel of the point to be estimated and “borrowed” area from the other tassels from the existing points. The 1-m resolution DTM was resampled to 3, 5, 10, 20, and 30 m grid cell resolution by using the mean aggregation function in order to obtain coarser DTMs.

4. Cell Size Dependence of Threshold Conditions

Numerical experiments are carried out to investigate the dependence of threshold conditions for the delineation of the drainage network on the grid cell size of the DTMs involved. For each channel head surveyed in the field, the related values of critical variables for channel initiation such as the drainage area A_t , the slope area relation AS_t^k with $k = 2$, the gradient divergence normalized by mean gradient D_t , the Strahler order SO_t , and the Horton order HO_t were determined by considering surface flow paths obtained from the application of the D8 and D8-LTD flow direction algorithms to DTMs of variable resolution. Mean and standard deviation of the critical variables computed over the 16 observed channel heads are shown in Fig. 3 in terms of data points and uncertainty bars, respectively, for all the considered grid cell sizes. Plots on the left hand side of Fig. 3 (a, c, e, g, and i) describe the results obtained from the D8 flow direction algorithm, while plots reported on the right hand side of Fig. 3 (b, d, f, h, and j) describe the results obtained from the D8-LTD algorithm. The method of weighted least squares described in Orlandini et al. (2006) is applied to determine predictive models of the variations of critical variables with grid cell size. Linear models are used to predict the variation of A_t , AS_t^k , and D_t with grid cell size h . Simple power function relationships are used to predict the variations of thresholds in terms of Strahler SO_t and Horton HO_t orders with h . The method of weighted least squares is applied to variable transformed logarithmically (base 10) in these cases. Predictive relationships are shown in Fig. 3 and reported in Table 1 along with the related coefficient of determination R^2 .

The results shown in Fig. 3 reveal a progressive increase of values of critical A_t and AS_t^k as the grid cell size increases (plots a, b, c, and d). The linear models reported in Table 1 display satisfactory coefficients of determination R^2 , especially when the D8-LTD algorithms is considered. The values of critical D_t at 1 m grid cell size displays a high uncertainty compared to the values obtained on coarser DTMs. This point does not significantly affect the predictive model obtained by weighted least square fitting and the resulting critical D_t is found to be practically constant. Under these circumstances the coefficient of determination R^2 does not provide high values as shown in Table 1. The plots related to the elaborations carried out with the critical SO_t and HO_t show a progressive decrease of thresholds order for channel initiation as the grid cell size increases. The SO_t is found to follow a power function relationship of grid cell size quite well, displaying a value R^2 equal to 1.00 when the D8 algorithm is applied, and equal to 0.99 when the D8-LTD algorithm is applied. This result appears noteworthy and suggests further investigations.

It is noted here that the results shown in Fig. 3 provide useful indications on the ability to identify threshold values that do not change significantly from one observed channel head to the others. These indications are provided by standard deviations used to compute uncertainty bars. In addition, these results illustrate the variations of threshold conditions as grid cell size varies. It is specified that the capability of a given criteria to identify a well defined threshold variable and the related variability with grid cell size does not necessarily ensure the ability of that criteria to predict accurately the drainage network. In fact, a well-identified criteria can provide predictions of channel heads in locations where these head does not occur and the predictive capabilities of criteria need to be evaluated separately. This evaluation is reported below.

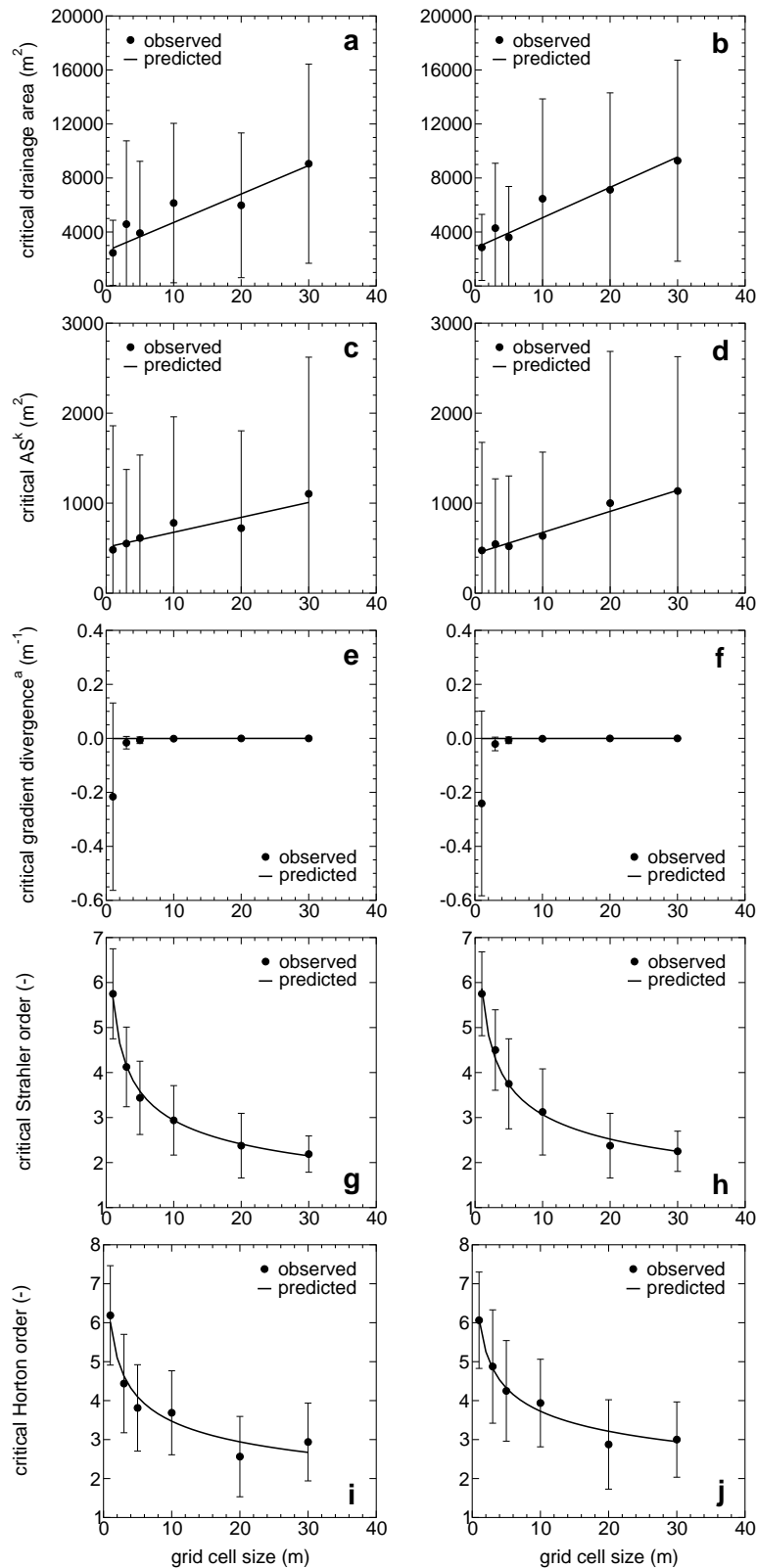


Figure 3. Observed and predicted values of critical variables for channel initiation as functions of grid cell size. Means (data points) and standard deviations (uncertainty bars) over the observed channel heads are provided for each grid cell size. Predictive relationships are obtained by weighted least squares fitting. Flow directions are determined by using the D8 (plots a, c, e, g, and i) and the D8-LTD (plots b, d, f, h, and j) flow direction algorithms.

5. Prediction of the Drainage Networks

The mean values of critical variables for channel initiation shown in the Fig. 3 have been used to extract the drainage networks from DTMs having variable resolution. In Fig. 4 the drainage networks determined using the various kind of critical variables and the D8 (maps on the left hand side) and D8-LTD (maps on the right hand side) flow direction algorithms are shown. The drainage networks extracted using the A_t (Fig. 4a and 4b) and SO_t (Fig. 4g and 4h) methods are found to reproduce satisfactorily the blue lines shown in Fig. 1. The best drainage network is obtained by considering the Strahler classification of the drainage network extracted directly from DTM data and pruning the exterior links with order less than or equal to $SO_t = 4$ (Fig. 4h). One can note that the agreement between predicted and observed channels is significantly less satisfactory when the D8 flow direction algorithm is used instead of the D8-LTD flow direction algorithm. The drainage networks extracted using the D8 algorithm provide predictions of channels in places where channels are not observed in the field nor reported in terms blue lines (Fig. 1). This is likely to indicate a poor ability of the D8 flow direction algorithm to describe surface flow paths along headwaters (e.g., Orlandini et al. 2003; Orlandini and Moretti 2009).

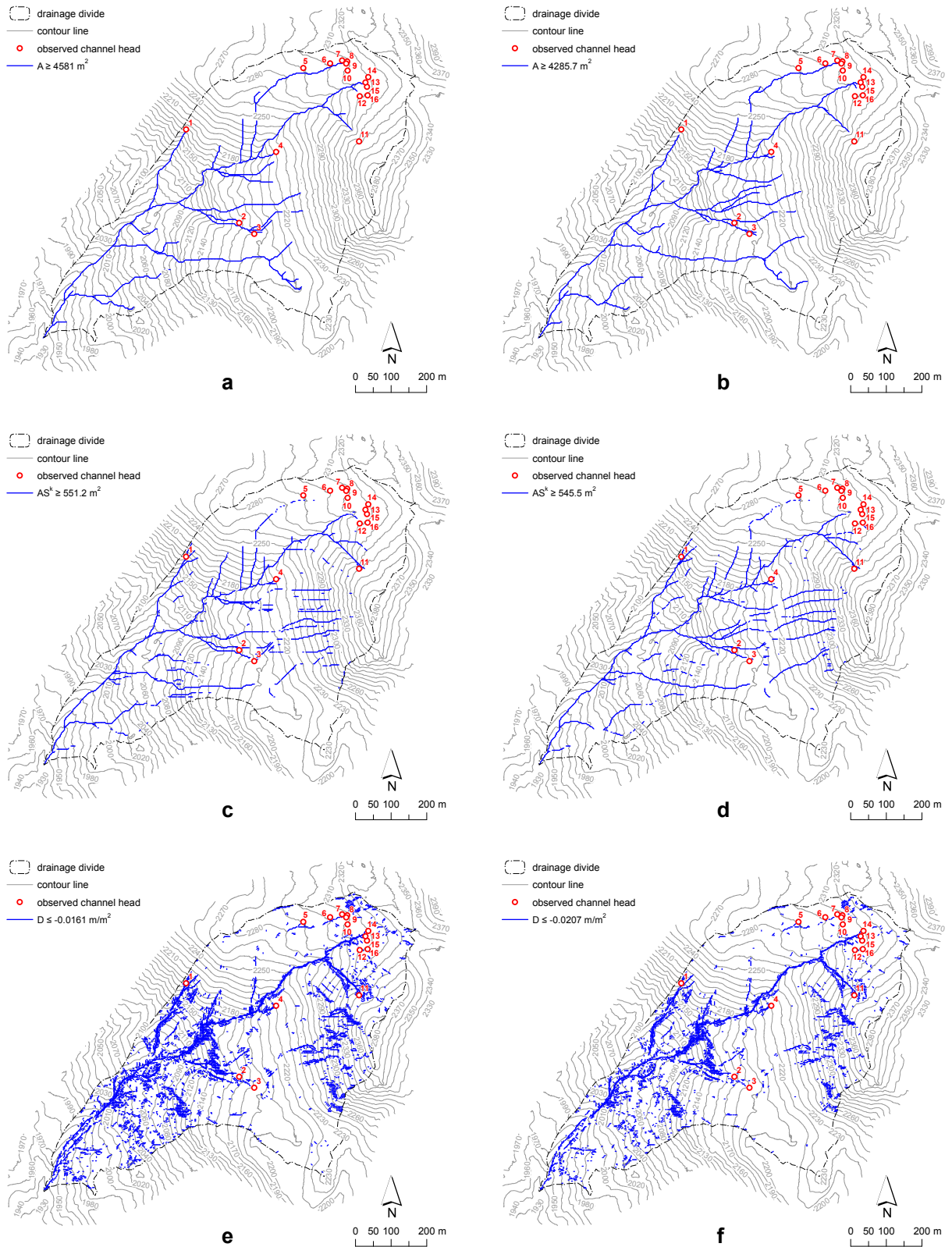
Fig. 4i and 4j show the drainage networks predicted by using the HO_t method. In the Horton classification, a channel of any order extends headward to the place the most distant tip ends, near the basin divide. In the case of D8-LTD algorithm the main channel follows a different path (Fig. 4j, near channel head #11) respect to the main channel reported in other maps. Once again, this reflects a different pattern of surface flow paths identified by the D8-LTD method and by the D8 method.

The drainage net extracted with AS_t^k (Fig. 4c and 4d) is well-identified along the steep valleys with all flow direction algorithms. This is not true when one looks at gently sloping areas where channel heads 5, 6, 7, 8, 9 and 10 are located. Here the channel is not recognized due to lower values of slope. It is noted that this approach strongly depends on the values of the local slope S , and in place where gentle slopes prevail seems not to be very reliable. The D_t method is found to provide a complex pattern of predicted channel heads that poorly reproduces the observed channel heads (Fig. 4e and 4f). These results suggests that this method predicts accurately the valleys but may not distinguish accurately the conditions in which channels occur.

Critical Variable for Channel Initiation	Flow Direction Method	Predictive Model as a Linear or Power Function of Grid Cell Size h (m)	
		Equation	R^2
Drainage area, A_t (m^2)	D8	$A_t = 2594.678 + 210.852 h$	0.87
Drainage area, A_t (m^2)	D8-LTD	$A_t = 2806.613 + 224.895 h$	0.92
AS_t^k (m^2)	D8	$AS_t^k = 510.531 + 16.579 h$	0.81
AS_t^k (m^2)	D8-LTD	$AS_t^k = 439.712 + 23.461 h$	0.96
Gradient divergence ^a , D_t (m^{-1})	D8	$D_t = -0.001 + 0.000 h$	0.30
Gradient divergence ^a , D_t (m^{-1})	D8-LTD	$D_t = -0.001 + 0.000 h$	0.21
Strahler order, SO_t	D8	$SO_t = 5.669 h^{-0.285}$	1.00
Strahler order, SO_t	D8-LTD	$SO_t = 5.869 h^{-0.282}$	0.99
Horton order, HO_t	D8	$HO_t = 6.018 h^{-0.239}$	0.95
Horton order, HO_t	D8-LTD	$HO_t = 6.095 h^{-0.214}$	0.98

^aGradient divergence normalized by mean gradient.

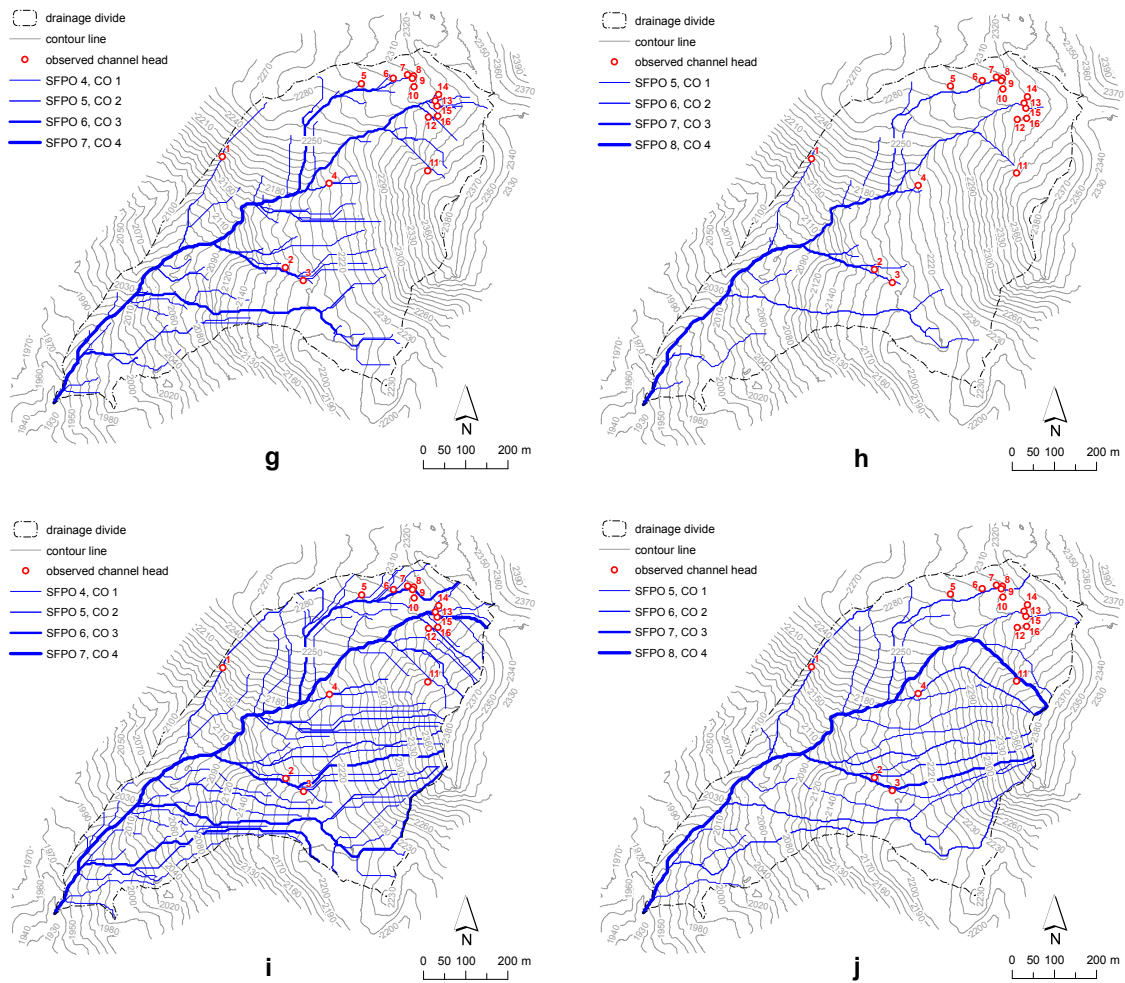
Table 1. Predictive models of the critical variables for channel initiation.



(continues)

Figure 4. Drainage networks obtained from 3-m resolution gridded elevation data by using the D8 and D8-LTD flow direction methods. The networks were extracted using the threshold for each critical variable for channel initiation (Fig. 3).

(continued)



6. Summary and Conclusions

This paper presented an analysis of the dependence of threshold conditions for the delineation of drainage networks from DTM on grid cell size. Two methods for the identification of flow direction were considered: the D8 and the D8-LTD methods. Five critical variables were considered for channel initiation: A_t , AS^k , D_t , SO_t , and HO_t . The results indicated that: (i) the threshold criteria for the channel initiation are grid cell size dependent, (ii) the critical variables A_t and SO_t for channel initiation are found to provide robust predictions of drainage networks from gridded elevation data, (iii) the SO_t method is found to follow well a scaling relation of grid cell size, and it represents therefore a good option for scaling analysis (upscaling and downscaling) related to drainage network identification, (iv) in some cases the use of the D8-LTD flow direction algorithm in preference to the D8 flow direction algorithm is critical in order to adequately describe surface flow paths along headwaters and the related channel heads. Future work will be carried out to test other methodologies for drainage network extraction based on the pure and semi-automatic geomorphometric approaches (Lashermes et al., 2008; Tarolli and Dalla Fontana, 2009), in order to provide a comprehensive view on dependence of threshold conditions for the delineation of drainage networks from grid cell size.

References

- Carter WE, Shrestha RL and Slatton KC, 2007, Geodetic laser scanning. *Physics Today*, 60(12): 41-47, doi:10.1063/1.2825070.
- Cavalli M, Tarolli P, Marchi L and Dalla Fontana G, 2008, The effectiveness of airborne LiDAR data in the recognition of channel bed morphology. *Catena*, 73: 249-260.
- Dietrich WE and Dunne T, 1993, The channel head. In: Beven K and Kirkby MJ (eds), *Channel Network Hydrology*. Wiley, New York, 175-219.
- Frankel KL and Dolan JF, 2007, Characterizing arid region alluvial fan surface roughness with airborne laser swath mapping digital topographic data. *J. Geophys. Res.*, 112: F02025, doi:10.1029/2006JF000644.
- Gallant JC and Wilson JP, 2000, Primary topographic attributes. In: Wilson JP and Gallant JC (eds), *Terrain Analysis: Principles and Applications*. Wiley, New York, 51-85.
- Glenn NF, Streutker DR, Chadwick DJ, Tahckray GD, and Dorsch SJ, 2006, Analysis of LIDAR-derived topography information for characterizing and differentiating landslide morphology and activity. *Geomorphology*, 73: 131-148.
- Horton RE, 1945, Erosional development of streams and their drainage basins: hydrophysical approach to quantitative morphology. *Bulletin of the Geological Society of America*, 56(3): 275-370.
- Howard AD, 1994, A detachment-limited model of drainage basin evolution. *Water Resources Research*, 30(7): 2261-2285.
- Lashermes B, Foufoula-Georgiou E and Dietrich WE, 2007, Channel network extraction from high resolution topography using wavelets. *Geophys. Res. Lett.*, 34: L23S04.
- Leopold LB, 1994, *A View of the River*. Harvard University Press, Cambridge, MA, USA.
- Leopold LB, Wolman MG and Miller JP, 1964, *Fluvial Processes in Geomorphology*. WH Freeman, San Francisco, CA, USA.
- Mckean J and Roering J, 2004, Objective landslide detection and surface morphology mapping using high-resolution airborne laser altimetry. *Geomorphology*, 57: 331-351, doi:10.1016/S0169-555X(03)00164-8.
- Montgomery DR and Dietrich WE, 1988, Where do channels begin? *Nature*, 336(6196): 232-234.
- Moretti G and Orlandini S, 2008, Automatic delineation of drainage basins from contour elevation data using skeleton construction techniques. *Water Resources Research*, 44: W05403, doi: 10.1029/2007WR006309.
- O'Callaghan J and Mark DM, 1984, The extraction of drainage networks from digital elevation data, *Computer Vision, Graphics, and Image Processing*, 28(3), 323-344.
- Orlandini S and Moretti G, 2009, Determination of surface flow paths from gridded elevation data. *Water Resources Research*, 45, W03417, doi: 10.1029/2008WR007099.
- Orlandini S, Boaretti C, Guidi V and Sfondrini G, 2006, Field determination of the spatial variation of resistance to flow along a steep Alpine stream, *Hydrol. Process.*, 20(18), 3897-3913, doi: 10.1002/hyp.6163.
- Orlandini S, Moretti G, Franchini M, Aldighieri B and Testa B, 2003, Path-based methods for the determination of nondispersive drainage directions in grid-based digital elevation models. *Water Resources Research*, 39(6): 1144, doi: 10.1029/2002WR001639.
- Peckham SD, 1995, Self-similarity in the three-dimensional geometry and dynamics of large river basins, PhD Thesis, University of Colorado, Boulder.
- Sibson R, 1981, A brief description of natural neighbor interpolation. *Interpreting Multivariate Data*. V. Barnett (eds) John Wiley: Chichester; 21-36.
- Strahler AN, 1957, Quantitative analysis of watershed geomorphology. *Transactions of the American Geophysical Union*, 38(6): 913-920.
- Tarboton G, Bras RL and Rodriguez-Iturbe I, 1988, The fractal nature of river networks. *Water Resources Research*, 24(8): 1317-1322.
- Tarolli P, Borga M and Dalla Fontana G, 2008, Analyzing the influence of upslope bedrock outcrops on shallow landsliding. *Geomorphology*, 93: 186-200, doi:10.1016/j.geomorph.2007.02.017.
- Tarolli P and Dalla Fontana G, 2009, Hillslope-to-valley transition morphology: new opportunities from high resolution DTMs. *Geomorphology*, doi:10.1016/j.geomorph.2009.02.006.
- Tarolli P and Tarboton DG, 2006, A new method for determination of most likely landslide initiation points and the evaluation of digital terrain model scale in terrain stability mapping. *Hydrol. Earth Syst. Sci.*, 10: 663-677.
- Vianello A, Cavalli M and Tarolli P, 2009, LiDAR-derived slopes for headwater channel network analysis. *Catena*, 76, 97-106, doi:10.1016/j.catena.2008.09.012.